

INVICTUS: Optimizing Boolean Logic Circuit Synthesis via Synergistic Learning and Search

Animesh B. Chowdhury*
New York University

Marco Romanelli
New York University

Benjamin Tan
University of Calgary

Ramesh Karri
New York University

Siddharth Garg
New York University

Abstract

Logic synthesis is the first and most vital step in chip design. This step converts a chip specification written in a hardware description language (such as Verilog) into an optimized implementation using Boolean logic gates. State-of-the-art logic synthesis algorithms have a large number of logic minimization heuristics, typically applied sequentially based on human experience and intuition. The choice of the order greatly impacts the quality (e.g., area and delay) of the synthesized circuit. In this paper, we propose INVICTUS, a model-based offline reinforcement learning (RL) solution that automatically generates a sequence of logic minimization heuristics ("synthesis recipe") based on a training dataset of previously seen designs. A key challenge is that new designs can range from being very similar to past designs (e.g., adders and multipliers) to being completely novel (e.g., new processor instructions). INVICTUS is the first solution that uses a mix of RL and search methods joint with an online out-of-distribution detector to generate synthesis recipes over a wide range of benchmarks. Our results demonstrate significant improvement in area-delay product (ADP) of synthesized circuits with up to 30% improvement over state-of-the-art techniques. Moreover, INVICTUS achieves up to $6.3\times$ runtime reduction (iso-ADP) compared to the state-of-the-art.

1 Introduction

Modern chips are designed using sophisticated electronic design automation (EDA) algorithms that automate the conversion of the description of a function, for example, in a hardware description language (HDL) like Verilog or VHDL, to a physical layout that can be manufactured at a semiconductor foundry. EDA involves a sequence of steps, the first of which is *logic synthesis*: this step converts a high-level HDL chip description into a low-level "netlist" of Boolean logic gates that implements the desired function. A netlist is a graph whose nodes are logic gates (e.g., ANDs, NOTs, ORs) and whose edges represent wires or connections between gates. Subsequent EDA steps, referred to as physical design, place gates in the netlist in a chip layout and route wires between them.

EDA tools seek to optimize quality metrics like area, delay, and power consumption of the final chip. As the first step in the EDA flow, the quality of the netlist produced by logic synthesis is crucial for the quality of all downstream steps and the final chip design. Beginning with an unoptimized netlist implementing a design, state-of-art logic synthesis algorithms perform a sequence of functionality-preserving transformations such as redundant node elimination, reordering Boolean formulas, and streamlining node representations, to arrive at a final optimized netlist [1–5] (see Figure 1). A specific sequence of transformations is called a "**synthesis recipe**." Typically, designers use experience and

*Corresponding authors: abc586@nyu.edu, sg175@nyu.edu

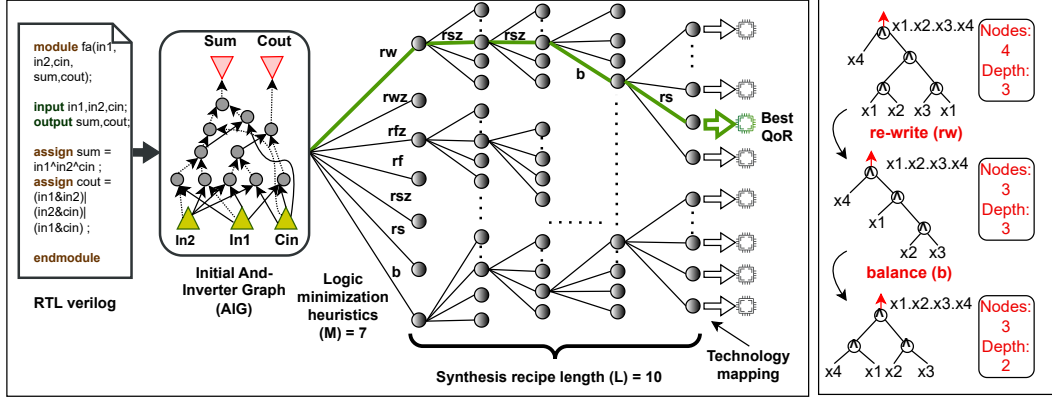


Figure 1: (Left) A hardware design in Verilog is first transformed into an and-inverter-graph (AIG), i.e., a netlist containing only AND and NOT gates. Then a sequence of functionality-preserving transformations (here, picked from set $\{rw, rwz, \dots, b\}$) is applied to generate an optimized AIG. Each such sequence is called a synthesis recipe. The optimized AIG is “technology-mapped” to a larger set of Boolean logic gates, producing the final netlist. The synthesis recipe with the best quality of result (QoR) (e.g., area or delay) is shown in green. (Right) Applying rw and b to an AIG results results in an optimized AIG with fewer nodes and lower depth.

intuition to pick a “good” synthesis recipe from the solution space of all recipes and iterate if the quality of result is poor. This manual process is costly and time-consuming, especially for modern, complex chips.

Recent work has explored the use of machine learning and reinforcement learning (RL) [6–18] to rapidly explore the solution space at different stages of the EDA flow, including for identifying high-quality synthesis recipes [15–17, 4, 5, 18]. One line of work [4, 5] proposes heuristic search methods, Monte-Carlo tree search (MCTS) in particular, to smartly explore the solution space for a given design. Although [4, 5] trains an agent during iterations of MCTS, these methods do *not* learn from historical data—public or private repositories of past designs that are abundant in semiconductor companies and increasingly on the internet [19]. Recent work [18] has shown that a predictive QoR model trained on past data in conjunction with simulated annealing-based search can outperform prior search-only methods.

Here we propose INVICTUS, a new approach that synergistically leverages both learning and search to rapidly identify high-quality synthesis recipes for a new design. INVICTUS has three main components: (1) a pre-trained offline RL agent trained on a dataset of past designs; (2) RL agent-guided MCTS search over the synthesis recipe space for new designs; and (3) when new designs are novel with respect to the training set, out-of-distribution (OOD) to select between the learned policy and pure search. Via ablations, we show that all three components, learning, search, and OOD, are critical for high-quality results. OOD detection, in particular, reflects real-world semiconductor design—new designs use a mix of previously seen modules (adders, multipliers, communication buses etc.) while also including novel functionality. We find these trends reflected in standard logic synthesis benchmark sets.

Evaluated on standard MCNC [20] and EPFL [21] benchmarks, INVICTUS achieves up to 10% and 30% reductions in area-delay product (ADP) compared to the state-of-the-art [5, 18]. Conversely, INVICTUS achieves the same ADP as prior work upto $6.3\times$ faster compared to [5] at iso-ADP. INVICTUS successfully classified all out-of-distribution (OOD) benchmarks in MCNC and EPFL(except one) further pushing the area-delay product (ADP) reduction upto 7%.

2 Proposed Approach

2.1 Problem Statement

We begin by formally defining the optimization problem we seek to solve. The definition is in the context of ABC [22], the leading open-source logic synthesis tool that also forms the basis of commercial tools. As shown in Figure 1, ABC first converts a Verilog description into an unoptimized

AIG, i.e., a graph $G_0 \in \mathcal{G}$, where \mathcal{G} is the set of all finite directed, acyclic, and bi-colored graphs. Note that since these attributes end-up having no bearing on the problem, we will not discuss them further. Next, ABC performs a functionality-preserving transformation on G_0 . We view these as a finite set of M actions, $\mathcal{A} = \{\text{rf}, \text{rm}, \dots, \text{b}\}$ (see §A.2 for more details). For ABC, $M = 7$. Applying an action on an AIG yields a new AIG as determined by the synthesis function $\mathbf{S} : \mathcal{G} \times \mathcal{A} \rightarrow \mathcal{G}$. Finally, a synthesis recipe $R \in \mathcal{A}^L$ is a sequence of L actions that are applied to G_0 in order. Given a synthesis recipe $P = \{a_0, a_1, \dots, a_{L-1}\}$ ($a_i \in \mathcal{A}$), then we obtain $G_{i+1} = \mathbf{S}(G_i, a_i)$ for all $i \in [0, L-1]$ where G_L is the final optimized AIG.

Finally, let $\mathbf{QoR} : \mathcal{G} \rightarrow \mathbb{R}$ measure the quality of graph G , for instance, its inverse area-delay product (so larger is better). Then, we seek to solve the following optimization problem:

$$\operatorname{argmax}_{P \in \mathcal{A}^L} \mathbf{QoR}(G_L), \text{ s.t. } G_{i+1} = \mathbf{S}(G_i, a_i) \forall i \in [0, L-1]. \quad (1)$$

We now discuss INVICTUS, our proposed approach to solve this optimization problem. We note that in addition to G_0 , the AIG to be synthesized, we will assume access to a training set of AIGs that can be used to aid optimization.

2.2 Baseline MCTS-based Optimization

The tree-structured solution space motivated prior work [4, 5] to adopt an MCTS-based approach that we briefly review here. A state s in this setting is an input AIG G_0 and sequence of $l \leq L$ actions, i.e., $\{a_0, a_1, \dots, a_l\}$. In a given state, any action $a \in \mathcal{A}$ can be picked as described above. Finally, the reward $\mathbf{QoR}(G_L)$ is delayed to the final synthesis step.

While we refer the reader to past work [4, 5] for more details. In iteration k of the search, Monte Carlo tree search (MCTS) keeps track of two functions: $Q_{MCTS}^k(s, a)$ which is measure the “goodness” of a state action pair, and $U_{MCTS}^k(s, a)$ which represents upper confidence tree (UCT) factor that encourages exploration of unseen or less visited states and actions. Exploiting known good states is balanced against exploration by selecting a policy $\pi_{MCTS}^k(s)$ that depends on both factors:

$$\pi_{MCTS}^k(s) = \operatorname{argmax}_{a \in \mathcal{A}} (Q_{MCTS}^k(s, a) + U_{MCTS}^k(s, a)). \quad (2)$$

More details on how these terms are updated are presented in §A.3, but we note that over iterations of MCTS, the policy tends towards the optimal with the exploration factor reducing and the exploitation factor increasing.

2.3 RL-Agent Training and Architecture

RL-agent training: Building on the same principles as [23], INVICTUS improves MCTS by training a reinforcement learning (RL) agent on previously seen circuits so as to guide MCTS search on a new circuit to “good” parts of the search space. Specifically, we use a dataset of N_{tr} training circuits to learn a policy $\pi_\theta(s, a)$ that outputs the probability of taking action a in state s and approximates the pure MCTS policy on the training set. Here, θ represents the trainable parameters of the policy agent.

Given a new circuit, the upper confidence tree (UCT in Equation 2) of MCTS is biased towards favorable paths by computing a new $U_{MCTS}^{*k}(s, a)$ as:

$$U_{MCTS}^{*k}(s, a) = \pi_\theta(s, a) \cdot U_{MCTS}^k(s, a). \quad (3)$$

Here, the learned policy term $\pi_\theta(s, a)$ biases MCTS against exploring states that are learned to yield bad QoR, i.e., when $\pi_\theta(s, a)$ is small.

Policy $\pi_\theta(s, a)$ is learned using a cross-entropy loss between the learned policy and the MCTS policy over samples picked from a replay buffer. We outline the pseudocode for RL-training in the appendix (Algorithm 1).

Policy network architecture: Our policy network (Figure 2) takes two inputs, (1) an initial AIG G_0 , and (2) a sequence of $l \leq L$ actions taken thus far, and outputs a probability distribution over the next action. Because the two inputs are in different formats, the policy network has two parallel branches that learn embeddings of the AIG and partial recipe. These embeddings are then concatenated and followed by additional layers to produce the final output.

For the AIG input, we employ a 3-layer graph convolutional network (GCN) [24] architecture to represent the AIG as a netlist embedding (h_{AIG}). We use LeakyReLU as the activation function and apply batch normalization before each layer. (See appendix §B.1 for details.) For recipe embeddings, We used a pre-trained BERT (Bidirectional Encoder Representations from Transformers) [25] model to encode synthesis recipes. BERT embeddings capture the context of a sequence of minimization heuristics and concatenates it with the h_{AIG} . The concatenated outputs are passed through three additional fully-connected layers.

In contrast to previous research [18], we use BERT two primary reasons: 1) BERT’s capacity to retain the contextual relationships within a sequence of actions in a synthesis recipe, thanks to its transformer-based architecture. Its self-attention mechanism is capable of discerning and encoding the inter-dependencies among various steps in the action sequence. 2) It can process variable-length inputs, producing fixed-length outputs, aligning with our requirements for generating consistent vector representations.

2.4 Synergistic Learning and Search

As we noted before, hardware designs frequently contain familiar and entirely new components. While we expect the learned RL-agent to help significantly on inputs similar to those in the training data, learning can hurt performance on novel inputs by biasing search towards low QoR regions of the search space.

Thus, we propose an out-of-distribution (OOD) solution for using MCTS with pre-trained agents: i.e., we use MCTS search with pre-trained agent if the new design is in-distribution with respect to training data, and otherwise, use pure MCTS.

Specifically, we use the cosine distance metric ($\Delta_{cos}(h_{k_1}, h_{k_2}) = 1 - \frac{h_{k_1} \cdot h_{k_2}}{\|h_{k_1}\| \|h_{k_2}\|}$) between the learned AIG representations of AIGs G_1 and G_2 to measure distance between AIGs. To modulate the balance between the prior learned policy and pure search, we update the UCT terms with a hyper-parameter $\alpha \in [0, 1]$ as follows: $U_{MCTS}^{*k}(s, a) = \pi_{\theta}(s, a)^{\alpha} \cdot U_{MCTS}^k(s, a)$. When $\alpha = 0$ the policy network is turned off and we implicitly default to pure search. Alternately when $\alpha = 1$ we revert to the prior learning and search-based solution. Although we later discuss how α can potentially be set to any value between 0 and 1, our proposed solution sets α to a binary value based on cosine distance:

$$\alpha = \begin{cases} 1 & \delta_{test}^{min} < \delta_{th}, \\ 0 & otherwise. \end{cases} \quad (4)$$

where threshold δ_{test}^{min} is the smallest cosine distance between the test input and AIGs in the training dataset, i.e., $\min_{h_i \in D_{train}} \Delta_{cos}(h_{test}, h_i)$, and δ_{th} is determined based on validation data. Specifically, we run each design in the validation set using the RL-agent guided and pure search. We then set δ_{th} to maximize geometric mean performance on the validation set.

Figure 6 outlines the proposed INVICTUS flow. Here, h_k indicates AIG embedding of design k . Cosine distance measures the similarity of two embeddings. For an unseen design G_{test} , we obtain its AIG embedding h_{test} by passing it through our pre-trained agent. We then measure $\Delta_{cos} h_{test}$ to the embeddings of designs used in training. We consider the cosine distance with the closest embedding Equation 4 to decide how to proceed: with standard MCTS or Agent-guided search.

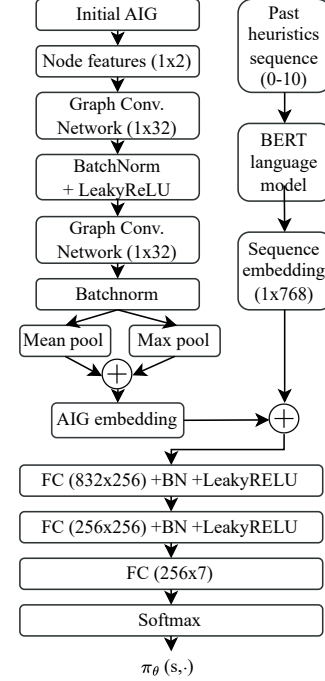


Figure 2: Policy network architecture. BN: Batch Normalization, FC: Fully connected layer

Table 1: Datasets used in our work

| Dataset | Splits | Circuits |
|----------------|--------|--------------------------------------------------------------------------------------------------------|
| MCNC | Train | alu2, apex3, apex5, b2, C1355, C5315, C2670, prom2, frg1, i7, i8, m3, max512, table5 |
| | Valid | apex7, c1908, c3540, frg2, max128, apex6, c432, c499, seq, table3, i10 |
| | Test | pair, max1024, alu4, apex1, apex2, apex4, c6288, c7552, i9, m4, prom1, b9, c880 |
| EPFL arith | I | Train: adder, div, log2, sin, sqrt, multiplier, max Test: square, bar |
| | II | Train: max, square, bar, div, sin, multiplier Test: adder, sqrt, log2 |
| | III | Train: adder, div, log2, sqrt, max, square, bar Test: multiplier, sin |
| | IV | Train: adder, log2, sqrt, square, bar, multiplier, sin Test: div, max |
| EPFL random | I | Train: cavlc, ctrl, dec, i2c, int2float, mem_ctrl, priority, router Test: arbiter, voter |
| | II | Train: arbiter, ctrl, i2c, int2float, mem_ctrl, priority, voter Test: cavlc, router |
| | III | Train: arbiter, cavlc, i2c, int2float, mem_ctrl, router, voter Test: ctrl, priority |
| | IV | Train: arbiter, cavlc, ctrl, i2c, int2float, priority, router, voter Test: mem_ctrl |
| | V | Train: arbiter, cavlc, ctrl, dec, mem_ctrl, priority, router, voter Test: i2c, int2float |

3 Empirical Evaluation

We present our experimental setup and compare INVICTUS against state-of-the-art (SOTA) methods on ADP and runtime reductions.

3.1 Experimental Setup

Datasets: We consider three popular datasets used by the logic synthesis community: MCNC [20], EPFL arithmetic and EPFL random control benchmarks [21]. MCNC benchmarks have 38 circuits ranging from 100 to 8000 node AIGs. EPFL benchmarks are of two different types: arithmetic and random control. The EPFL arithmetic benchmarks perform operations like additions, multiplications etc. and have between 1000-44000 nodes. These benchmarks share common sub-modules, for examples, multipliers are typically implemented by stacking adders. Finally, the EPFL random control benchmarks consist of finite-state machines, routing logic and other random functions with between 100 to 46000 nodes.

Train-test split: We train dataset-specific RL agents to evaluate performance of INVICTUS using train-validation-test splits motivated by [26]. The splits used for each dataset are discussed below:

1. **MCNC:** We divide MCNC dataset circuits into three sets (Table 1): training, validation and test sets. The training set contains 14 circuits; validation and test data consists of 12 circuits each. We train a single MCNC agent since it is the largest benchmark suite and provides sufficiently many circuits for training, validation and test.
2. **EPFL arithmetic:** We create four variants of the EPFL arithmetic benchmark suite. In the first three variants, we train arithmetic agents I, II and III using a 7-2 split of training and test data. Arithmetic agent IV is trained using a 6-3 split of training and test data. This strategy ensures that each of the nine EPFL arithmetic circuits appears in atleast one (in fact exactly one) test set, thus allowing us to report results on each circuit in the benchmark suite. The splits are performed randomly. For validation data, we combine training circuits for each agent with unseen circuits from the MCNC benchmark suite (alu2 and apex7), along with four EPFL control circuits. We use validation data to set δ_{th} (OOD hyperparameter).
3. **EPFL random control:** Similar to arithmetic benchmarks, we divide random control benchmarks into four 7-2 split and one 8-1 split and train five RL agents. We create validation data following the above strategy.

Optimization objective and metrics: We seek to identify the best $L = 10$ synthesis recipes. Consistent with prior works [16, 17, 5], we use area-delay product (ADP) as evaluation metric. Area and delay values are obtained using a 7nm technology library post technology mapping of the synthesized AIG. As a baseline, we compare against the ADP of the resyn2 synthesis recipe as is also done in prior work [5, 18]. In addition to ADP reduction, we also report runtime reduction of INVICTUS at iso-ADP, i.e., how much faster INVICTUS is in reaching the best ADP achieved by competing methods.

Training details and hyper-parameters: We present our network architecture in Figure 2. We use He initialization [27] for the weights of our RL agents. Following [28], we multiply the weights of the final layer with 0.01 to prevent bias towards any action. We train our agents for 50 epochs. We used the Adam optimizer set the initial learning rate to 0.01.

In each epoch, we perform MCTS on each training circuit. The MCTS search budget (K) is set to 512 at each level of synthesis. At each level, the replay buffer stores the best experience tuple having information about the state and action probability distribution scores collected from Monte Carlo rollouts. After performing MCTS simulations on training circuits, we sample $L \times N_{tr}$ (N_{tr} is the number of training circuits) experiences from the replay buffer (of size $2 \times L \times N_{tr}$) to train the agent. The RL agent minimizes the cross entropy loss between π_θ and the MCTS agent π_{MCTS} . To stabilize training, we normalize our QoR rewards (see Appendix C.1) and clip it to $[-1, +1]$ [29].

We performed the training on a server machine with one NVIDIA RTX A4000 with 16GB VRAM. The major bottleneck during training is the synthesis time for running ABC; actual gradient updates are relatively inexpensive. Agent training took around 27 hours for MCNC and 7 days for EPFL arithmetic and random control.

Evaluation: We compare INVICTUS with three main methods: (1) standard MCTS [5]; (2) MCTS augmented with an RL agent trained on-line (i.e., on the circuit being optimized) but not on past training data [17]; and (3) simulated annealing (SA) with QoR predictor learned from training data [18]. Methods (1) and (3) and SA are the current SOTA methods. For completeness, we also compare with (2) although it has already been shown to underperform (1). During evaluations on test circuits, we give each technique a budget of 100 synthesis runs.

| Designs | ADP reduction (in %) | | | | | Iso-ADP Speed-Up |
|-----------|----------------------|----------------|--------------|--------------|-----------------|------------------|
| | Online-RL [17] | SA+ Pred. [18] | MCTS [5] | INVICTUS | | |
| | | | | $\alpha = 1$ | +OOD | |
| alu4 | 20.61 | 17.58 | 17.05 | 21.95 | 21.95(✓) | 4.5x |
| apex1 | 6.58 | 17.01 | 15.95 | 17.54 | 17.54(✓) | 2.6x |
| apex2 | 8.12 | 15.58 | 13.06 | 17.51 | 17.51(✓) | 4.7x |
| apex4 | 13.53 | 13.01 | 13.01 | 13.95 | 13.95(✓) | 3.2x |
| i9 | 39.35 | 46.45 | 46.89 | 53.97 | 53.97(✓) | 1.6x |
| m4 | 20.95 | 18.16 | 14.98 | 20.05 | 20.05(✓) | 1.7x |
| prom1 | 4.97 | 8.53 | 6.50 | 11.23 | 11.23(✓) | 2.5x |
| b9 | 17.92 | 23.65 | 23.21 | 24.10 | 24.10(✓) | 6.3x |
| c880 | 16.23 | 19.95 | 17.75 | 24.58 | 24.58(✓) | 6.3x |
| c7552 | 20.21 | 17.62 | 20.45 | 12.78 | 20.45(✗) | 1.0x |
| pair | 4.73 | 10.02 | 13.10 | 12.65 | 13.10(✗) | 1.0x |
| max1024 | 11.39 | 20.27 | 19.65 | 18.32 | 19.65(✗) | 1.0x |
| Geomean | 12.80 | 17.34 | 16.66 | 18.84 | 19.76 | 2.5x |
| Win ratio | 1/12 | 1/12 | 2/12 | 8/12 | 10/12 | 9/12 |

3.2 Results

We now discuss the performance of INVICTUS in reducing area-delay product and improving run-time over state-of-the-art.

MCNC benchmarks: Figure 3 demonstrates the effectiveness of INVICTUS generated recipes over SOTA methods [17, 5, 18] in terms of percentage ADP reduction (all relative to resyn2) and iso-ADP speedup. We report data for INVICTUS without ($\alpha = 1$) and with our OOD strategy. Recall that without OOD, INVICTUS uses a mix of learning and search. With OOD, however, INVICTUS defaults to pure MCTS on OOD inputs. We also report the overall win ratio, i.e., the number of circuits on which a particular method achieves the best results. The results show that on 10 out of 12 benchmarks, INVICTUS generates better recipes than standard MCTS [5] and SA with QoR prediction (SA+Pred.) [18], with substantial improvements on benchmarks such as alu4, apex2, i9, m4, prom1, and c880. INVICTUS’s geo. mean improvements (with OOD) are also the highest overall. Finally, note that INVICTUS’s OOD detector correctly defaults to pure search in all three cases where pure MCTS outperforms INVICTUS’s history-based RL-guided search.

Figure 3 plots the ADP reductions over search iterations for MCTS, SA+Pred, and INVICTUS ($\alpha = 1$, or equivalently without OOD). In alu4, INVICTUS’s agent explores paths with higher rewards whereas standard MCTS continues searching without further improvement. A similar trend is observed for apex2, m4, prom1 demonstrating that a pre-trained agent helps bias search towards better parts of the search space. SA+Pred. [18] also leverages past history, but is unable to compete (on average) with MCTS and INVICTUS in part because SA typically underperforms MCTS on tree-based search spaces.

Also note from Figure 3 that INVICTUS in most cases achieves higher ADP reductions earlier than competing methods. This results in significant run-time speedups of $2.5\times$ at iso-ADP compared

Table 2: Area-delay reduction over resyn2 on MCNC benchmarks. ✓ denotes INVICTUS used RL agent during search whereas X denotes standard MCTS

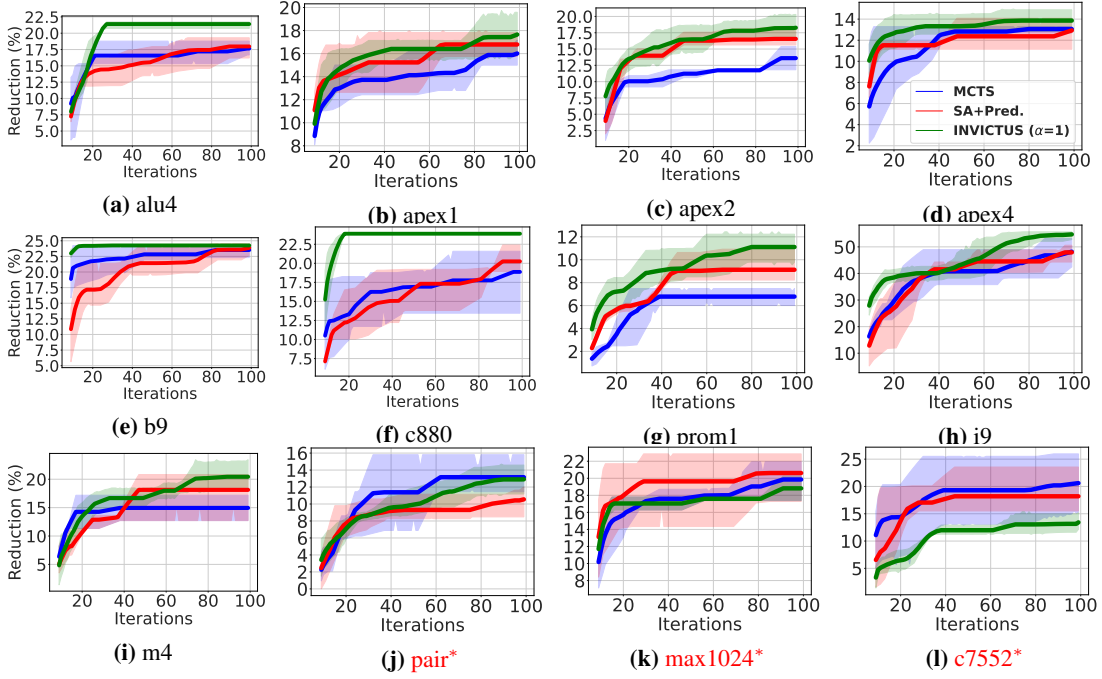


Figure 3: Area-delay product reduction (in %) compared to resyn2 on MCNC circuits. INVICTUS classified c7552, pair and max1024 as out-of-distribution samples and defaults to pure MCTS search. For rest of the circuits, INVICTUS performs pre-trained RL agent-guided search.

to standard MCTS [5]. On in-distribution benchmarks, the speed-up is as high as $6.3\times$; on OOD benchmarks INVICTUS performs standard MCTS resulting in the same speed as prior work.

EPFL arithmetic benchmarks:

Table 3 presents the ADP reduction achieved by INVICTUS and competing methods on EPFL arithmetic circuits. On these benchmarks, we correctly classified all except for the square benchmark as in-distribution. Additionally, INVICTUS wins on all nine benchmarks, using OOD detection to match up to pure MCTS on square. Overall, INVICTUS achieved a geom. mean ADP reduction of 22.07% over resyn2, representing improvements of +5.52% and +6.93% over standard MCTS and SA+Pred., respectively. Finally, INVICTUS achieves on an average $1.6\times$ runtime speed-up at iso-ADP compared to standard MCTS [5], with up to $6.3\times$ speed-up in the best case (Figure 4).

EPFL random control benchmarks:

Table 4 presents the ADP reduction achieved by INVICTUS and competing methods on EPFL random control circuits. Although our overall conclusions are the same, i.e., INVICTUS outperforms competing methods, the trends for this benchmark set are different. First, INVICTUS’s OOD detector is triggered for four of the five benchmark circuits, which is more frequent than for prior benchmark sets. This aligns with the variability in circuit structure and functionality within the EPFL random control benchmark characterization [21], causing different synthesis recipe behaviors and train-test distribution shifts. In the case of router, the OOD detector is triggered incorrectly, i.e., for this benchmark leveraging the pre-trained RL agent would have been helpful.

| Designs | ADP reduction (in %) | | | | | Iso-ADP Speed-Up |
|------------|----------------------|----------------|--------------|--------------|-----------------|------------------|
| | Online-RL [17] | SA+ Pred. [18] | MCTS [5] | INVICTUS | | |
| | | | | $\alpha = 1$ | +OOD | |
| adder | 18.63 | 18.63 | 18.63 | 18.63 | 18.63(✓) | 2.2x |
| bar | 36.89 | 36.89 | 25.37 | 36.89 | 36.89(✓) | 0.6x |
| div | 34.83 | 25.16 | 45.94 | 55.64 | 55.64(✓) | 1.4x |
| log2 | 4.73 | 9.58 | 9.09 | 11.51 | 11.51(✓) | 1.9x |
| max | 25.09 | 29.87 | 37.50 | 46.86 | 46.86(✓) | 1.2x |
| multiplier | 12.41 | 9.75 | 9.90 | 12.68 | 12.68(✓) | 1.4x |
| sin | 5.57 | 14.30 | 14.50 | 15.96 | 15.96(✓) | 2.4x |
| square | 10.44 | 8.20 | 12.28 | 9.75 | 12.28(X) | 1.0x |
| sqrt | 24.10 | 21.10 | 18.69 | 24.24 | 24.24(X) | 6.3x |
| Geomean | 15.41 | 17.01 | 18.42 | 21.51 | 22.07 | 1.6x |
| Win ratio | 2/9 | 2/9 | 2/9 | 8/9 | 9/9 | 7/9 |

Table 3: Area-delay reduction over resyn2 on EPFL arithmetic benchmarks. ✓ denotes INVICTUS perform agent guided search whereas X denotes standard MCTS

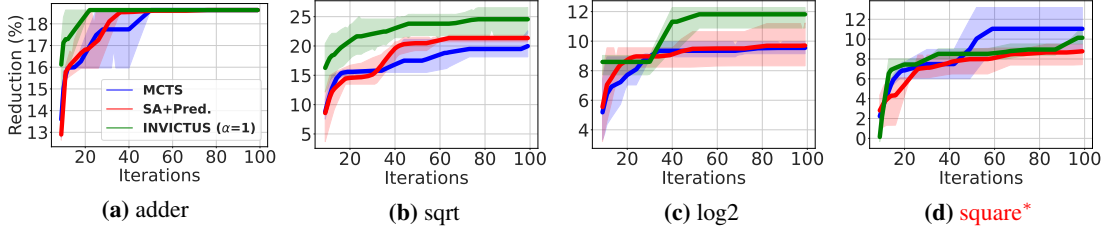


Figure 4: Area-delay product reduction (in %) compared to resyn2 on EPFL arithmetic circuits. INVICTUS classified square as out-of-distribution samples and defaults to pure MCTS search. For rest of the circuits, INVICTUS performs pre-trained RL agent-guided search.

INVICTUS’s pre-trained RL agent is useful for the remaining five benchmarks; outperforming standard MCTS [5] and simulated annealing with QoR predictor [18] in each case. INVICTUS also wins overall on seven of nine benchmarks. INVICTUS loses once to SA+Pred. and, interestingly, once to itself without OOD detection. Finally, INVICTUS achieves on an average $1.5\times$ iso-ADP runtime speed-up compared to standard MCTS [5] with a maximum speed-up of $3\times$.

| Designs | ADP reduction (in %) | | | | | Iso-ADP Speed-Up |
|-----------|-----------------------|----------------------|--------------|--------------|-------------------|---------------------|
| | Online- RL [17] | SA+ Pred. [18] | MCTS [5] | INVICTUS | | |
| | | | | $\alpha = 1$ | +OOD | |
| arbiter | 0.03 | 0.03 | 0.03 | 0.03 | 0.03(✓) | 2.4x |
| cavlc | 16.28 | 16.75 | 15.85 | 13.89 | 15.85(✗) | 1.0x |
| ctrl | 22.97 | 25.85 | 27.58 | 30.85 | 30.85(✓) | 2.6x |
| i2c | 14.91 | 13.10 | 13.45 | 15.65 | 15.65(✓) | 3.0x |
| int2float | 7.41 | 7.52 | 8.10 | 7.52 | 8.10(✗) | 1.0x |
| mem_ctrl | 22.54 | 21.45 | 21.55 | 23.67 | 23.67(✓) | 2.1x |
| priority | 74.62 | 77.10 | 77.53 | 75.10 | 77.53(✗) | 1.0x |
| router | 10.71 | 27.53 | 21.63 | 25.68 | 21.63(✗) | 1.0x |
| voter | 8.26 | 26.45 | 27.10 | 26.05 | 27.10(✗) | 1.0x |
| Geomean | 8.29 | 10.47 | 10.38 | 10.69 | 10.80 | 1.5x |
| Win ratio | 0/9 | 2/9 | 4/9 | 5/9 | 7/9 | 4/9 |

4 Discussion and Limitations

We now discuss opportunities to improve INVICTUS and its limitations.

Our results so far indicate that for OOD designs, defaulting to a pure search strategy outperforms RL-guided search. However, this assumes a binary assignment to the α parameter in Equation 4. Smoothly varying α enables the extent of learning used in search to be varied. To this end: we modified Equation 4 to a more generalized function as follows:

$$\alpha = 1 - \frac{1}{1 + \exp\left(-\frac{\delta_{test}^{min} - \delta_{th}}{T}\right)} \quad (5)$$

Here, we introduce temperature T to smoothen our α to real valued function in range $[0, 1]$. Setting $T = 0$ leads to Equation 4. We call this soft OOD and tune T on our validation dataset and present our results in Table 5. Overall, smoothening α yields better geometric mean and win ratio for MCNC and EPFL random control circuits, but falls behind slightly on EPFL arithmetic benchmarks.

Figure 5 outlines the performance of smoothing on out-of-distribution benchmarks from MCNC and EPFL random control. We obtain ADP reduction upto 4.7% on top of pure MCTS search. This highlights an important insight: a small factor of trained agent’s recommendation help bias search towards favourable paths. One strong possibility of such improved performance can be attributed to recipes learned by the agent which broadly works well across different designs. Our future studies include detailed investigation of α smoothing instead of hard OOD based decision making and its explainability. We believe synergistically combining learning and search is going to help yield better results under time-to-market pressure in EDA industry.

Table 4: Area-delay reduction compared to resyn2 on EPFL random-control benchmarks. ✓denotes INVICTUS deploy agent guided search whereas X denotes standard MCTS

| Settings | MCNC | | EPFL arith | | EPFL random | |
|--------------|-------|-------|------------|------|-------------|------|
| | G.M. | W.R. | G.M. | W.R. | G.M. | W.R. |
| $\alpha = 1$ | 18.84 | 8/12 | 21.46 | 8/9 | 10.78 | 5/9 |
| $T = 0$ | 19.76 | 10/12 | 22.07 | 9/9 | 10.80 | 7/9 |
| $T = 0.06$ | 20.41 | 11/12 | 21.63 | 8/9 | 11.32 | 7/9 |

Table 5: Varying agent’s recommendation during search

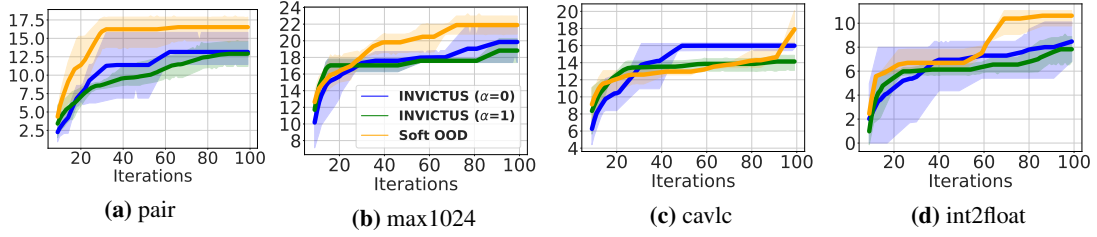


Figure 5: Area-delay product reduction (in %) using soft OOD versus hard OOD on out-of-distribution samples

Limitations: INVICTUS also has some limitations. First, large, standardized, open-source datasets are scarce in the hardware community. Our results suggest that RL agents can be effectively trained on few training circuits (although note that for each circuit we generate thousands of synthesis runs), but evaluations on larger scale datasets will be illuminating. To that point, INVICTUS’s training is costly, running into a week for our benchmarks. Interestingly, the bottleneck is the cost of repeatedly running logic synthesis during training; mitigating training time is an area of future improvement. Finally, INVICTUS does not address the challenge of continually updating the learned policy agent as new designs are seen.

5 Related work

Prior work in logic synthesis can be classified into three categories: expert-crafted synthesis recipes [1–3], classical optimization approaches [4, 5] and learning-guided approaches [13–18]. In the first category, researchers have studied the transformations performed by logic minimization heuristics on a variety of circuit benchmarks and devised “good” synthesis recipes (e.g. `resyn2` [2]) which tend to perform reasonably on a wide range of benchmarks. We show that to get good results, synthesis recipes must be tailored to the design. Classical optimization techniques [4, 5] formulate the logic synthesis problem as a black-box optimization problem and leverage heuristics such as MCTS to generate design-specific synthesis recipes. Compared to these methods, we show that learning from previous designs can improve quality and run-time.

Learning-based approaches can further be classified into two sub-categories: 1) Synthesis recipe classification [15, 14] and prediction [19, 18] based approaches, and 2) RL-based approaches [13, 16, 17]. In [15], the authors train a CNN classifier to classify an unseen synthesis recipe as “angel” or “devil” recipe using a QoR labeled dataset generated by synthesizing the design. [14] partition the original graph into smaller sub-networks and performs binary classification on sub-networks to pick which recipes work best. However, these methods only work over a small number of pre-selected recipes and have been outperformed by MCTS search methods. [18, 19] learns a QoR predictor model for a given AIG and synthesis recipe using a massive synthesis dataset and use it with simulated annealing for larger search space exploration within a specified time budget. On the other hand, RL-based solutions [13, 16, 17] use online RL algorithms to craft synthesis recipes, but do not leverage any prior data. We show that INVICTUS outperforms these methods.

Finally, ML has been deployed for a range of other EDA problems as well [6–12, 30]. Closer to this work, [6] trains a deep-RL agent to optimize chip floorplanning, a different EDA problem that seeks to place modules of a synthesized design on the surface of a chip. Compared to logic synthesis, each action in floorplanning, i.e., moving the x-y coordinates of modules in the design, is computationally inexpensive, unlike the time-consuming actions in logic synthesis. Thus, a large number of moves can be simulated even on a new design, enabling the trained agent to be fine-tuned. INVICTUS uses a different strategy, synergistically combining learning and search with an out-of-distribution detector.

6 Conclusion

We propose INVICTUS, a novel approach that combines learning, search, and out-of-distribution (OOD) detection that greatly improves the process of identifying high-quality synthesis recipes for new hardware designs. Particularly, the integrated use of a pre-trained RL agent, an RL agent-guided

MCTS search over the synthesis recipe space, and an OOD selection process between the learned policy and pure search has proved to be effective. These keys ideas backed by empirical results highlight the potential of INVICTUS to generate high-quality synthesis recipes making modern complex chips design more efficient and cost-effective.

References

- [1] Wenlong Yang, Lingli Wang, and Alan Mishchenko. Lazy man’s logic synthesis. In *Proceedings of the International Conference on Computer-Aided Design*, pages 597–604, 2012.
- [2] Alan Mishchenko, Satrajit Chatterjee, and Robert Brayton. DAG-aware aig rewriting: A fresh look at combinational logic synthesis. In *Design Automation Conference (DAC)*, pages 532–535, 2006.
- [3] Heinz Riener, Eleonora Testa, Winston Haaswijk, Alan Mishchenko, Luca Amarù, Giovanni De Micheli, and Mathias Soeken. Scalable generic logic synthesis: One approach to rule them all. In *Proceedings of the 56th Annual Design Automation Conference 2019*, pages 1–6, 2019.
- [4] Cunxi Yu. Flowtune: Practical multi-armed bandits in boolean optimization. In *International Conference On Computer Aided Design (ICCAD)*, pages 1–9, 2020.
- [5] Walter Lau Neto, Yingjie Li, Pierre-Emmanuel Gaillardon, and Cunxi Yu. Flowtune: End-to-end automatic logic optimization exploration via domain-specific multi-armed bandit. *IEEE Transactions on Computer-Aided Design of Integrated Circuits and Systems*, 2022.
- [6] Azalia Mirhoseini, Anna Goldie, Mustafa Yazgan, Joe Wenjie Jiang, Ebrahim Songhori, Shen Wang, Young-Joon Lee, Eric Johnson, Omkar Pathak, Azade Nazi, et al. A graph placement methodology for fast chip design. *Nature*, 594(7862):207–212, 2021.
- [7] Vitaly Kurin, Saad Godil, Shimon Whiteson, and Bryan Catanzaro. Can q-learning with graph networks learn a generalizable branching heuristic for a sat solver? *Advances in Neural Information Processing Systems*, 33:9608–9621, 2020.
- [8] Yao Lai, Yao Mu, and Ping Luo. Maskplace: Fast chip placement via reinforced visual representation learning. *Advances in Neural Information Processing Systems*, 35:24019–24030, 2022.
- [9] Frederik Schmitt, Christopher Hahn, Markus N Rabe, and Bernd Finkbeiner. Neural circuit synthesis from specification patterns. *Advances in Neural Information Processing Systems*, 34:15408–15420, 2021.
- [10] Emre Yolcu and Barnabás Póczos. Learning local search heuristics for boolean satisfiability. *Advances in Neural Information Processing Systems*, 32, 2019.
- [11] Shobha Vasudevan, Wenjie Joe Jiang, David Bieber, Rishabh Singh, C Richard Ho, Charles Sutton, et al. Learning semantic representations to verify hardware designs. *Advances in Neural Information Processing Systems*, 34:23491–23504, 2021.
- [12] Zhihao Yang, Dong Li, Yingxueff Zhang, Zhanguang Zhang, Guojie Song, Jianye Hao, et al. Versatile multi-stage graph neural network for circuit representation. *Advances in Neural Information Processing Systems*, 35:20313–20324, 2022.
- [13] Winston Haaswijk, Edo Collins, Benoit Seguin, Mathias Soeken, Frédéric Kaplan, Sabine Süssstrunk, and Giovanni De Micheli. Deep learning for logic optimization algorithms. In *International Symposium on Circuits and Systems (ISCAS)*, pages 1–4, 2018.
- [14] Walter Lau Neto, Max Austin, Scott Temple, Luca Amaru, Xifan Tang, and Pierre-Emmanuel Gaillardon. LSOracle: a logic synthesis framework driven by artificial intelligence: Invited paper. In *International Conference on Computer-Aided Design (ICCAD)*, pages 1–6, 2019.
- [15] Cunxi Yu, Houping Xiao, and Giovanni De Micheli. Developing synthesis flows without human knowledge. In *Design Automation Conference (DAC)*, pages 1–6, 2018.
- [16] Abdelrahman Hosny, Soheil Hashemi, Mohamed Shalan, and Sherief Reda. DRiLLS: Deep reinforcement learning for logic synthesis. In *Asia and South Pacific Design Automation Conference (ASP-DAC)*, pages 581–586, 2020.
- [17] Keren Zhu, Mingjie Liu, Hao Chen, Zheng Zhao, and David Z. Pan. Exploring logic optimizations with reinforcement learning and graph convolutional network. In *Workshop on Machine Learning for CAD (MLCAD)*, pages 145–150, 2020.

- [18] Animesh Basak Chowdhury, Benjamin Tan, Ryan Carey, Tushit Jain, Ramesh Karri, and Siddharth Garg. Bulls-eye: Active few-shot learning guided logic synthesis. *IEEE Transactions on Computer-Aided Design of Integrated Circuits and Systems*, 2022.
- [19] Animesh Basak Chowdhury, Benjamin Tan, Ramesh Karri, and Siddharth Garg. Openabc-d: A large-scale dataset for machine learning guided integrated circuit synthesis. *arXiv preprint arXiv:2110.11292*, 2021.
- [20] Saeyang Yang. *Logic synthesis and optimization benchmarks user guide: version 3.0*. Citeseer, 1991.
- [21] Luca Amarú, Pierre-Emmanuel Gaillardon, and Giovanni De Micheli. The epfl combinational benchmark suite. In *Proceedings of the 24th International Workshop on Logic & Synthesis (IWLS)*, number CONF, 2015.
- [22] Robert Brayton and Alan Mishchenko. ABC: An Academic Industrial-Strength Verification Tool. In Tayssir Touili, Byron Cook, and Paul Jackson, editors, *Computer Aided Verification*, pages 24–40, 2010.
- [23] David Silver, Aja Huang, Chris J Maddison, Arthur Guez, Laurent Sifre, George Van Den Driessche, Julian Schrittwieser, Ioannis Antonoglou, Veda Panneershelvam, Marc Lanctot, et al. Mastering the game of go with deep neural networks and tree search. *nature*, 529(7587):484–489, 2016.
- [24] Thomas N Kipf and Max Welling. Semi-supervised classification with graph convolutional networks. *arXiv preprint arXiv:1609.02907*, 2016.
- [25] Jacob Devlin, Ming-Wei Chang, Kenton Lee, and Kristina Toutanova. Bert: Pre-training of deep bidirectional transformers for language understanding. *arXiv preprint arXiv:1810.04805*, 2018.
- [26] Justin Fu, Aviral Kumar, Ofir Nachum, George Tucker, and Sergey Levine. D4rl: Datasets for deep data-driven reinforcement learning. *arXiv preprint arXiv:2004.07219*, 2020.
- [27] Kaiming He, Xiangyu Zhang, Shaoqing Ren, and Jian Sun. Delving deep into rectifiers: Surpassing human-level performance on imagenet classification. In *Proceedings of the IEEE international conference on computer vision*, pages 1026–1034, 2015.
- [28] Marcin Andrychowicz, Anton Raichuk, Piotr Stańczyk, Manu Orsini, Sertan Girgin, Raphael Marinier, Léonard Hussenot, Matthieu Geist, Olivier Pietquin, Marcin Michalski, et al. What matters in on-policy reinforcement learning? a large-scale empirical study. *arXiv preprint arXiv:2006.05990*, 2020.
- [29] Volodymyr Mnih, Koray Kavukcuoglu, David Silver, Andrei A Rusu, Joel Veness, Marc G Bellemare, Alex Graves, Martin Riedmiller, Andreas K Fidjeland, Georg Ostrovski, et al. Human-level control through deep reinforcement learning. *nature*, 518(7540):529–533, 2015.
- [30] Chung-Kuan Cheng, Andrew B Kahng, Sayak Kundu, Yucheng Wang, and Zhiang Wang. Assessment of reinforcement learning for macro placement. In *Proceedings of the 2023 International Symposium on Physical Design*, pages 158–166, 2023.
- [31] Robert K Brayton, Gary D Hachtel, Curt McMullen, and Alberto Sangiovanni-Vincentelli. *Logic minimization algorithms for VLSI synthesis*, volume 2. Springer Science & Business Media, 1984.
- [32] Levente Kocsis and Csaba Szepesvári. Bandit based monte-carlo planning. In *Machine Learning: ECML 2006: 17th European Conference on Machine Learning Berlin, Germany, September 18-22, 2006 Proceedings 17*, pages 282–293. Springer, 2006.

7 Reproducibility

We provide our detailed experimental setup and model hyperparameters in Section 3. We have shared the codes for training our model at the following URL: <https://anonymous.4open.science/r/invictus-83A3/>. Post acceptance of our work, we will publicly release it with detailed user’s instruction.

8 Broader Impact

Our work INVICTUS attempts to solve one of the main combinatorial optimization problem in the field of electronic design automation (EDA). We foresee our work to be adopted similarly in other optimization problems such as floorplanning, macro placement, routing and design rule checks. The ideas may nurture promising growth of machine learning (ML) in chip design automation: which is regarded is one of the most complex optimization problems and still rely a lot on experienced engineers and practitioners’ input to achieve better quality of result (QoR).

A Appendix 1

A.1 Logic Synthesis

Logic synthesis transforms a hardware design in register transfer level (RTL) to a Boolean gate-level network, optimizes the number of gates/depth, and then maps it to standard cells in a technology library [31]. Well-known representations of Boolean networks include sum-of-product form, product-of-sum, Binary decision diagrams, and AIGs which are a widely accepted format using only AND (nodes) and NOT gates (dotted edges). Several logic minimization heuristics (discussed in Section A.2)) have been developed to perform optimization on AIG graphs because of its compact circuit representation and directed acyclic graph (DAG)-based structuring. These heuristics are applied sequentially (“synthesis recipe”) to perform one-pass logic optimization reducing the number of nodes and depth of AIG. The optimized network is then mapped using cells from technology library to finally report area, delay and power consumption.

A.2 Logic minimization heuristics

We now describe optimization heuristics provided by industrial strength academic tool ABC [22]:

- 1. Balance (b)** optimizes AIG depth by applying associative and commutative logic function tree-balancing transformations to optimize for delay.
- 2. Rewrite (rw, rw -z)** is a directed acyclic graph (DAG)-aware logic rewriting technique that performs template pattern matching on sub-trees and encodes them with equivalent logic functions.
- 3. Refactor (rf, rf -z)** performs aggressive changes to the netlist without caring about logic sharing. It iteratively examines all nodes in the AIG, lists out the maximum fan-out-free cones, and replaces them with equivalent functions when it improves the cost (e.g., reduces the number of nodes).
- 4. Re-substitution (rs, rs -z)** creates new nodes in the circuit representing intermediate functionalities using existing nodes; and remove redundant nodes. Re-substitution improves logic sharing.

The zero-cost (-z) variants of these transformation heuristics perform structural changes to the netlist without reducing nodes or depth of AIG. However, previous empirical results show circuit transformations help future passes of other logic minimization heuristics reduce the nodes/depth and achieve the minimization objective.

A.3 Monte Carlo Tree Search

We discuss in detail the MCTS algorithm. During selection, a search tree is built from the current state by following a search policy, with the aim of identifying promising states for exploration.

where $Q_{MCTS}^k(s, a)$ denotes estimated Q value (discussed next) obtained after taking action a from state s during the k^{th} iteration of MCTS simulation. $U_{MCTS}^k(s, a)$ represents upper confidence tree (UCT) exploration factor of MCTS search.

$$U_{MCTS}^k(s, a) = c_{UCT} \sqrt{\frac{\log(\sum_a N_{MCTS}^k(s, a))}{N_{MCTS}^k(s, a)}}, \quad (6)$$

$N_{MCTS}^k(s, a)$ denotes the visit count of the resulting state after taking action a from state s . c_{UCT} denotes a constant exploration factor [32].

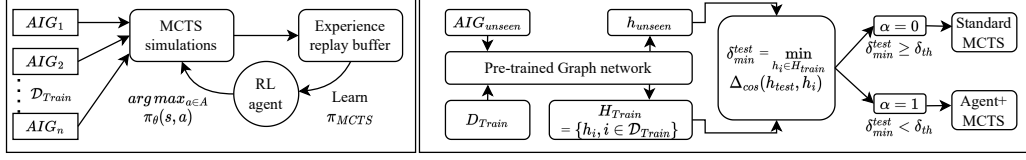


Figure 6: INVICTUS flow: Training the agent (left) and Recipe generation at inference-time (right)

The selection phase repeats until a leaf node is reached in the search tree. A leaf node in MCTS tree denotes either no child nodes have been created or it is a terminal state of the environment. Once a leaf node is reached the expansion phase begins where an action is picked randomly and its roll out value is returned or $R(s_L)$ is returned for the terminal state s_L . Next, back propagation happens where all parent nodes $Q_k(s, a)$ values are updated according to the following equation.

$$Q_{MCTS}^k(s, a) = \sum_{i=1}^{N_{MCTS}^k(s, a)} R_{MCTS}^i(s, a) / N_{MCTS}^k(s, a). \quad (7)$$

A.4 INVICTUS Agent Pre-Training Process

As discussed in Section 2.3, we pre-train an agent using available past data to help with choosing which logic minimization heuristic to add to the synthesis recipe. The process is shown as Algorithm 1.

Algorithm 1 Invictus: Policy agent pre-training

```

1: procedure TRAINING( $\theta$ )
2:   Replay buffer ( $RB$ )  $\leftarrow \phi$ ,  $\mathcal{D}_{train} = \{AIG_1, AIG_2, \dots, AIG_n\}$ , num_epochs= $N$ , Recipe
   length= $L$ , AIG embedding network:  $\Lambda$ , Recipe embedding network:  $\mathcal{R}$ , Agent policy  $\pi_\theta := U$ 
   (Uniform distribution), MCTS iterations =  $K$ , Action space =  $A$ 
3:   for  $AIG_i \in \mathcal{D}_{train}$  do
4:      $r \leftarrow 0$ ,  $depth \leftarrow 0$ 
5:      $s \leftarrow \Lambda(AIG_i) + \mathcal{R}(r)$ 
6:     while  $depth < L$  do
7:        $\pi_{MCTS} = MCTS(s, \pi_\theta, K)$ 
8:        $a = \operatorname{argmax}_{a' \in A} \pi_{MCTS}(s, a')$ 
9:        $r \leftarrow r + a$ ,  $s' \leftarrow \mathcal{A}(AIG_i) + \mathcal{R}(r)$ 
10:       $RB \leftarrow RB \cup (s, a, s', \pi_{MCTS}(s, \cdot))$ 
11:       $s \leftarrow s'$ ,  $depth \leftarrow depth + 1$ 
12:   for epochs  $< N$  do
13:      $\theta \leftarrow \theta_i - \alpha \nabla_\theta \mathcal{L}(\pi_{MCTS}, \pi_\theta)$ 

```

B Network architecture

B.1 AIG Network architecture

Starting with a graph $G = (\mathbf{V}, \mathbf{E})$ that has vertices \mathbf{V} and edges \mathbf{E} , the GCN aggregates feature information of a node with its neighbors' node information. The output is then normalized using Batchnorm and passed through a non-linear LeakyReLU activation function. This process is repeated for k layers to obtain information for each node based on information from its neighbours up to a distance of k -hops. A graph-level READOUT operation produces a graph-level embedding. Formally:

$$h_u^k = \sigma(W_k \sum_{i \in u \cup N(u)} \frac{h_i^{k-1}}{\sqrt{N(u)} \times \sqrt{N(v)}} + b_k), k \in [1..K] \quad (8)$$

$$h_G = \text{READOUT}(\{h_u^k; u \in V\})$$

The embedding for node u , generated by the k^{th} layer of the GCN, is represented by h_u^k . The parameters W_k and b_k are trainable, and σ is a non-linear ReLU activation function. $N(\cdot)$ denotes the 1-hop neighbors of a node. The READOUT function combines the activations from the k^{th} layer of all nodes to produce the final

output by performing a pooling operation. In our work, we choose $k = 2$ and global average and max pooling concatenated as READOUT operation.

C Experimental details

C.1 Reward normalization

In our work, maximizing QoR entails finding a recipe P which is minimizing the area-delay product of transformed AIG graph. We consider as a baseline recipe an expert-crafted synthesis recipe `resyn2` [2] on top of which we improve our ADP.

$$R = \begin{cases} 1 - \frac{ADP(S(G,P))}{ADP(S(G,resyn2))} & ADP(S(G,P)) < 2 \times ADP(S(G,P)), \\ -1 & otherwise. \end{cases}$$

D Results

D.1 EPFL arithmetic benchmarks

We used agent-based search to evaluate the ADP reduction on EPFL arithmetic benchmarks. We treated each circuit as test data and evaluated it with a corresponding RL agent. Figure 4 shows that, except for the `square` benchmark, agent-guided search minimized ADP more effectively than both standard MCTS [5] and simulated annealing [18]. This performance suggests that the pre-training circuits share similar characteristics with the test data circuits.

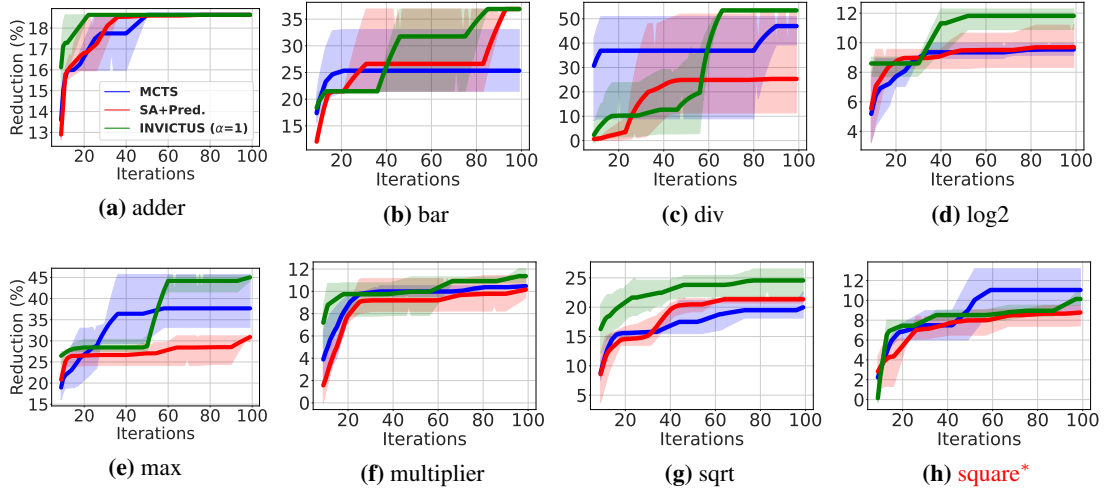


Figure 7: Area-delay product reduction (in %) compared to `resyn2` on EPFL arithmetic benchmarks. We evaluated `bar` and `square` with arithmetic agent I, `adder`, `sqrt` and `log2` with arithmetic agent II, `multiplier` and `sin` with arithmetic agent III and `div` and `max` with arithmetic agent IV. GREEN: INVICTUS ($\alpha = 1$), BLUE: MCTS [5], RED: SA+Pred. [18]

D.2 EPFL random control benchmarks

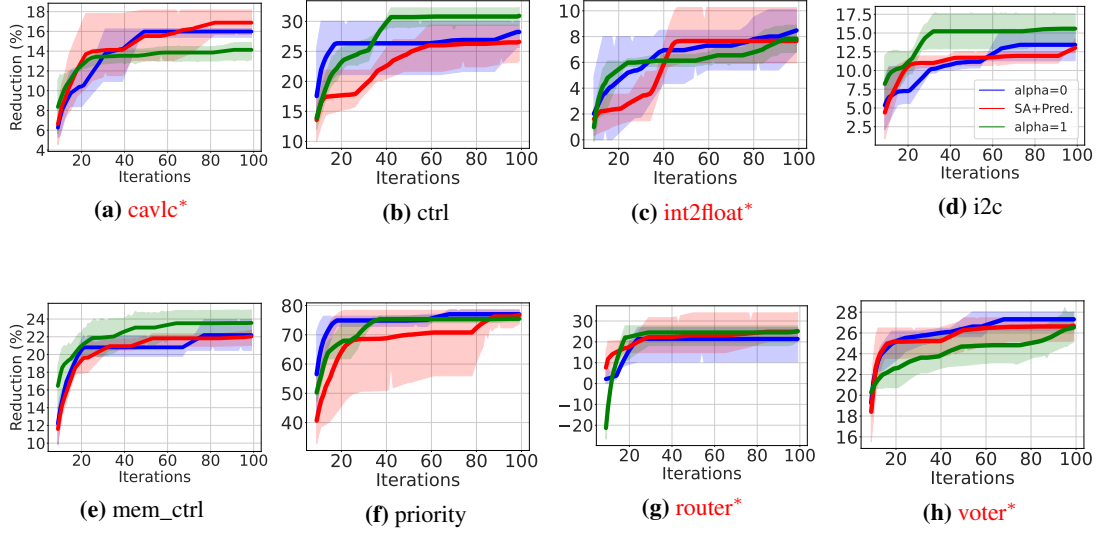


Figure 8: Area-delay product reduction (in %) compared to resyn2 on EPFL random control benchmarks. Except *router*, our OOD detector successfully identified the average winner approach. GREEN: INVICTUS ($\alpha = 1$), BLUE: MCTS [5], RED: SA+Pred. [18]

E Out-of-distribution detection

We use cosine distance (Δ_{cos}) based OOD detection to check similarity of a new “unseen” design bear with training designs embeddings. Next, we report δ_{th} obtained for various RL agents trained in our experiments using validation data. (See Section 3). Table 6 outlines the data for MCNC agent; Table 7, 8, 9 and 10 presents the data for EPFL arithmetic agents and Table 11, 12, 13, 14 and 15 report the numbers for EPFL random control agents.

Table 6: Δ_{cosine} on validation data (MCNC agent). δ_{th} computed from AUROC curve: 0.007

| Validation benchmarks | $\Delta_{cos}(h_{valid}, h_{train})$ | | | | | | | | | | | | | | δ_{min} | Winner (0-MCTS+RL / 1- MCTS) |
|-----------------------|--------------------------------------|-------|-------|-------|-------|-------|-------|-------|-------|-------|-------|-------|--------|--------|----------------|------------------------------|
| | alu2 | apex3 | apex5 | b2 | c1355 | c5315 | c2670 | prom2 | frg1 | i7 | i8 | m3 | max512 | table5 | | |
| apex7 | 0.003 | 0.046 | 0.016 | 0.042 | 0.041 | 0.016 | 0.019 | 0.07 | 0.04 | 0.052 | 0.048 | 0.026 | 0.025 | 0.032 | 0.003 | 0 |
| c1908 | 0.022 | 0.098 | 0.036 | 0.088 | 0.009 | 0.039 | 0.043 | 0.125 | 0.023 | 0.11 | 0.103 | 0.047 | 0.059 | 0.076 | 0.009 | 0 |
| c3540 | 0.002 | 0.04 | 0.02 | 0.033 | 0.034 | 0.016 | 0.019 | 0.059 | 0.029 | 0.053 | 0.045 | 0.017 | 0.016 | 0.026 | 0.002 | 0 |
| frg2 | 0.03 | 0.022 | 0.016 | 0.023 | 0.085 | 0.007 | 0.006 | 0.034 | 0.077 | 0.038 | 0.03 | 0.017 | 0.019 | 0.015 | 0.006 | 1 |
| max128 | 0.018 | 0.023 | 0.016 | 0.023 | 0.067 | 0.004 | 0.004 | 0.038 | 0.058 | 0.043 | 0.034 | 0.014 | 0.014 | 0.015 | 0.004 | 0 |
| apex6 | 0.018 | 0.071 | 0.025 | 0.063 | 0.033 | 0.026 | 0.029 | 0.094 | 0.033 | 0.081 | 0.076 | 0.032 | 0.043 | 0.053 | 0.018 | 1 |
| c432 | 0.009 | 0.034 | 0.04 | 0.025 | 0.042 | 0.025 | 0.025 | 0.041 | 0.026 | 0.067 | 0.052 | 0.008 | 0.013 | 0.024 | 0.008 | 1 |
| c499 | 0.03 | 0.124 | 0.064 | 0.112 | 0.006 | 0.059 | 0.055 | 0.153 | 0.012 | 0.147 | 0.136 | 0.069 | 0.078 | 0.1 | 0.006 | 1 |
| seq | 0.028 | 0.009 | 0.033 | 0.012 | 0.115 | 0.027 | 0.035 | 0.008 | 0.098 | 0.01 | 0.016 | 0.015 | 0.015 | 0.01 | 0.008 | 1 |
| table3 | 0.028 | 0.01 | 0.036 | 0.025 | 0.112 | 0.028 | 0.033 | 0.037 | 0.094 | 0.014 | 0.007 | 0.012 | 0.014 | 0.01 | 0.007 | 1 |
| i10 | 0.017 | 0.007 | 0.02 | 0.006 | 0.091 | 0.016 | 0.022 | 0.018 | 0.078 | 0.012 | 0.008 | 0.011 | 0.003 | 0.002 | 0.002 | 0 |

Table 7: Δ_{\cosine} on validation data (EPFL arithmetic agent I). δ_{th} computed from AUROC curve: 0.005

| Validation benchmarks | $\Delta_{\cos}(h_{valid}, h_{train})$ | | | | | | | δ_{min} | Winner (0-MCTS+RL /1- MCTS) |
|-----------------------|---------------------------------------|-------|-------|------------|-------|-------|-------|----------------|-----------------------------------|
| | adder | div | log2 | multiplier | sin | sqrt | max | | |
| adder_alu2 | 0.094 | 0.047 | 0.04 | 0.025 | 0.014 | 0.025 | 0.071 | 0.014 | 1 |
| div_alu2 | 0.228 | 0 | 0.001 | 0.004 | 0.011 | 0.005 | 0.112 | 0 | 0 |
| log2_alu2 | 0.219 | 0.001 | 0 | 0.002 | 0.008 | 0.004 | 0.051 | 0 | 0 |
| multiplier_alu2 | 0.182 | 0.004 | 0.002 | 0 | 0.002 | 0.001 | 0.009 | 0 | 0 |
| sin_alu2 | 0.152 | 0.012 | 0.008 | 0.003 | 0 | 0.003 | 0.011 | 0 | 0 |
| sqrt_alu2 | 0.173 | 0.005 | 0.004 | 0.001 | 0.002 | 0 | 0.004 | 0 | 0 |
| max_alu2 | 0.24 | 0.003 | 0.006 | 0.011 | 0.02 | 0.01 | 0.001 | 0.001 | 0 |
| | | | | | | | | | |
| adder_apex7 | 0.075 | 0.092 | 0.082 | 0.06 | 0.044 | 0.062 | 0.078 | 0.044 | 1 |
| div_apex7 | 0.228 | 0 | 0.001 | 0.004 | 0.011 | 0.005 | 0.094 | 0 | 0 |
| log2_apex7 | 0.219 | 0.001 | 0 | 0.002 | 0.008 | 0.004 | 0.056 | 0 | 0 |
| multiplier_apex7 | 0.182 | 0.004 | 0.002 | 0 | 0.002 | 0.001 | 0.011 | 0 | 0 |
| sin_apex7 | 0.153 | 0.011 | 0.008 | 0.002 | 0 | 0.003 | 0.019 | 0 | 0 |
| sqrt_apex7 | 0.175 | 0.004 | 0.003 | 0.001 | 0.002 | 0 | 0.008 | 0 | 0 |
| max_apex7 | 0.242 | 0.003 | 0.006 | 0.012 | 0.021 | 0.011 | 0.003 | 0.003 | 0 |
| | | | | | | | | | |
| arbiter | 0.123 | 0.059 | 0.049 | 0.034 | 0.023 | 0.037 | 0.049 | 0.023 | 1 |
| cavlc | 0.124 | 0.025 | 0.02 | 0.009 | 0.004 | 0.009 | 0.011 | 0.004 | 0 |
| priority | 0.014 | 0.21 | 0.2 | 0.163 | 0.131 | 0.157 | 0.043 | 0.014 | 1 |
| router | 0.25 | 0.492 | 0.478 | 0.449 | 0.414 | 0.448 | 0.024 | 0.25 | 1 |

Table 8: Δ_{\cos} on validation data (EPFL arithmetic agent II). δ_{th} computed from AUROC curve: 0.006

| Validation benchmarks | $\Delta_{\cos}(h_{valid}, h_{train})$ | | | | | | δ_{min} | Winner (0-MCTS+RL /1- MCTS) |
|-----------------------|---------------------------------------|-------|-------|------------|-------|--------|----------------|-----------------------------------|
| | bar | div | max | multiplier | sin | square | | |
| bar_alu2 | 0 | 0.005 | 0.014 | 0.009 | 0.018 | 0.071 | 0 | 0 |
| div_alu2 | 0.005 | 0 | 0.003 | 0.004 | 0.011 | 0.082 | 0 | 0 |
| max_alu2 | 0.014 | 0.003 | 0 | 0.011 | 0.02 | 0.112 | 0 | 0 |
| multiplier_alu2 | 0.009 | 0.004 | 0.011 | 0 | 0.002 | 0.054 | 0 | 0 |
| sin_alu2 | 0.018 | 0.012 | 0.021 | 0.003 | 0 | 0.043 | 0 | 0 |
| square_alu2 | 0.06 | 0.069 | 0.096 | 0.043 | 0.033 | 0.001 | 0.001 | 0 |
| | | | | | | | | |
| bar_apex7 | 0 | 0.005 | 0.014 | 0.009 | 0.018 | 0.071 | 0 | 0 |
| div_apex7 | 0.005 | 0 | 0.003 | 0.004 | 0.011 | 0.082 | 0 | 0 |
| max_apex7 | 0.014 | 0.003 | 0 | 0.012 | 0.021 | 0.113 | 0 | 0 |
| multiplier_apex7 | 0.009 | 0.004 | 0.011 | 0 | 0.002 | 0.055 | 0 | 0 |
| sin_apex7 | 0.018 | 0.011 | 0.02 | 0.002 | 0 | 0.044 | 0 | 0 |
| square_apex7 | 0.07 | 0.081 | 0.112 | 0.054 | 0.043 | 0 | 0 | 0 |
| | | | | | | | | |
| arbiter | 0.055 | 0.059 | 0.083 | 0.034 | 0.023 | 0.008 | 0.008 | 1 |
| cavlc | 0.051 | 0.047 | 0.064 | 0.025 | 0.014 | 0.018 | 0.014 | 1 |
| priority | 0.236 | 0.21 | 0.228 | 0.163 | 0.131 | 0.108 | 0.108 | 1 |
| router | 0.508 | 0.492 | 0.504 | 0.449 | 0.414 | 0.386 | 0.386 | 1 |

Table 9: Δ_{\cosine} on validation data (EPFL arithmetic agent III). δ_{th} computed from AUROC curve: 0.01

| Validation benchmarks | $\Delta_{\cos}(h_{valid}, h_{train})$ | | | | | | | δ_{min} | Winner (0-MCTS+RL /1- MCTS) |
|-----------------------|---------------------------------------|-------|-------|-------|-------|--------|-------|----------------|-----------------------------------|
| | adder | bar | div | log2 | max | square | sqrt | | |
| adder_alu2 | 0.094 | 0.051 | 0.047 | 0.04 | 0.064 | 0.01 | 0.025 | 0.01 | 0 |
| bar_alu2 | 0.257 | 0 | 0.005 | 0.004 | 0.014 | 0.071 | 0.012 | 0 | 0 |
| div_alu2 | 0.228 | 0.005 | 0 | 0.001 | 0.003 | 0.082 | 0.005 | 0 | 0 |
| log2_alu2 | 0.219 | 0.004 | 0.001 | 0 | 0.006 | 0.07 | 0.004 | 0 | 0 |
| max_alu2 | 0.24 | 0.014 | 0.003 | 0.006 | 0 | 0.112 | 0.01 | 0 | 0 |
| square_alu2 | 0.133 | 0.06 | 0.069 | 0.058 | 0.096 | 0.001 | 0.048 | 0.001 | 0 |
| sqrt_alu2 | 0.173 | 0.012 | 0.005 | 0.004 | 0.01 | 0.059 | 0 | 0 | 0 |
| | | | | | | | | | |
| adder_apex7 | 0.075 | 0.093 | 0.092 | 0.082 | 0.117 | 0.01 | 0.062 | 0.01 | 0 |
| bar_apex7 | 0.259 | 0 | 0.005 | 0.004 | 0.014 | 0.071 | 0.013 | 0 | 0 |
| div_apex7 | 0.228 | 0.005 | 0 | 0.001 | 0.003 | 0.082 | 0.005 | 0 | 0 |
| log2_apex7 | 0.219 | 0.004 | 0.001 | 0 | 0.006 | 0.07 | 0.004 | 0 | 0 |
| max_apex7 | 0.242 | 0.014 | 0.003 | 0.006 | 0 | 0.113 | 0.011 | 0 | 0 |
| square_apex7 | 0.14 | 0.07 | 0.081 | 0.07 | 0.112 | 0 | 0.059 | 0 | 0 |
| sqrt_apex7 | 0.175 | 0.012 | 0.004 | 0.003 | 0.01 | 0.059 | 0 | 0 | 0 |
| | | | | | | | | | |
| arbiter | 0.123 | 0.055 | 0.059 | 0.049 | 0.083 | 0.008 | 0.037 | 0.008 | 0 |
| cavlc | 0.124 | 0.03 | 0.025 | 0.02 | 0.038 | 0.027 | 0.009 | 0.009 | 0 |
| priority | 0.014 | 0.236 | 0.21 | 0.2 | 0.228 | 0.108 | 0.157 | 0.014 | 1 |
| router | 0.25 | 0.508 | 0.492 | 0.478 | 0.504 | 0.386 | 0.448 | 0.25 | 1 |

Table 10: Δ_{\cosine} on validation data (EPFL arithmetic agent IV). δ_{th} computed from AUROC curve: 0.01

| Validation benchmarks | $\Delta_{\cos}(h_{valid}, h_{train})$ | | | | | | | δ_{min} | Winner (0-MCTS+RL /1- MCTS) |
|-----------------------|---------------------------------------|-------|-------|------------|-------|--------|-------|----------------|-----------------------------------|
| | adder | bar | log2 | multiplier | sin | square | sqrt | | |
| adder_alu2 | 0.094 | 0.051 | 0.04 | 0.025 | 0.01 | 0.018 | 0.025 | 0.01 | 0 |
| bar_alu2 | 0.257 | 0 | 0.004 | 0.009 | 0.018 | 0.071 | 0.012 | 0 | 0 |
| log2_alu2 | 0.219 | 0.004 | 0 | 0.002 | 0.008 | 0.07 | 0.004 | 0 | 0 |
| multiplier_alu2 | 0.182 | 0.009 | 0.002 | 0 | 0.002 | 0.054 | 0.001 | 0 | 0 |
| sin_alu2 | 0.152 | 0.018 | 0.008 | 0.003 | 0 | 0.043 | 0.003 | 0 | 0 |
| square_alu2 | 0.133 | 0.06 | 0.058 | 0.043 | 0.033 | 0.001 | 0.048 | 0.001 | 0 |
| sqrt_alu2 | 0.173 | 0.012 | 0.004 | 0.001 | 0.002 | 0.059 | 0 | 0 | 0 |
| | | | | | | | | | |
| adder_apex7 | 0.075 | 0.093 | 0.082 | 0.06 | 0.044 | 0.01 | 0.062 | 0.01 | 0 |
| bar_apex7 | 0.259 | 0 | 0.004 | 0.009 | 0.018 | 0.071 | 0.013 | 0 | 0 |
| log2_apex7 | 0.219 | 0.004 | 0 | 0.002 | 0.008 | 0.07 | 0.004 | 0 | 0 |
| multiplier_apex7 | 0.182 | 0.009 | 0.002 | 0 | 0.002 | 0.055 | 0.001 | 0 | 0 |
| sin_apex7 | 0.153 | 0.018 | 0.008 | 0.002 | 0 | 0.044 | 0.003 | 0 | 0 |
| square_apex7 | 0.14 | 0.07 | 0.07 | 0.054 | 0.043 | 0 | 0.059 | 0 | 0 |
| sqrt_apex7 | 0.175 | 0.012 | 0.003 | 0.001 | 0.002 | 0.059 | 0 | 0 | 0 |
| | | | | | | | | | |
| arbiter | 0.123 | 0.055 | 0.049 | 0.034 | 0.023 | 0.008 | 0.037 | 0.008 | 0 |
| cavlc | 0.124 | 0.03 | 0.02 | 0.009 | 0.004 | 0.027 | 0.009 | 0.004 | 0 |
| priority | 0.014 | 0.236 | 0.2 | 0.163 | 0.131 | 0.108 | 0.157 | 0.014 | 1 |
| router | 0.25 | 0.508 | 0.478 | 0.449 | 0.414 | 0.385 | 0.448 | 0.25 | 1 |

Table 11: Δ_{\cosine} on validation data (EPFL random control agent I). δ_{th} computed from AUROC curve: 0.008

| Validation benchmarks | $\Delta_{\cos}(h_{valid}, h_{train})$ | | | | | | | δ_{min} | Winner (0-MCTS+RL /1- MCTS) |
|-----------------------|---------------------------------------|-------|-------|-----------|----------|----------|--------|----------------|-----------------------------------|
| | cavlc | ctrl | i2c | int2float | mem_ctrl | priority | router | | |
| cavlc_apex7 | 0.001 | 0.005 | 0.032 | 0.016 | 0.022 | 0.117 | 0.402 | 0.001 | 0 |
| ctrl_apex7 | 0.006 | 0.001 | 0.02 | 0.027 | 0.025 | 0.123 | 0.386 | 0.001 | 0 |
| i2c_apex7 | 0.037 | 0.023 | 0 | 0.062 | 0.051 | 0.153 | 0.393 | 0 | 0 |
| int2float_apex7 | 0.008 | 0.017 | 0.049 | 0.002 | 0.057 | 0.073 | 0.339 | 0.002 | 1 |
| mem_ctrl_apex7 | 0.029 | 0.031 | 0.051 | 0.072 | 0 | 0.233 | 0.498 | 0 | 0 |
| priority_apex7 | 0.031 | 0.047 | 0.088 | 0.005 | 0.108 | 0.042 | 0.314 | 0.005 | 0 |
| router_apex7 | 0.286 | 0.278 | 0.292 | 0.236 | 0.366 | 0.218 | 0.022 | 0.022 | 0 |
| | | | | | | | | | |
| cavlc_alu2 | 0 | 0.006 | 0.034 | 0.013 | 0.027 | 0.106 | 0.398 | 0 | 0 |
| ctrl_alu2 | 0.004 | 0.002 | 0.024 | 0.018 | 0.037 | 0.096 | 0.377 | 0.002 | 0 |
| i2c_alu2 | 0.035 | 0.022 | 0 | 0.059 | 0.052 | 0.146 | 0.391 | 0 | 0 |
| int2float_alu2 | 0.007 | 0.017 | 0.049 | 0.001 | 0.059 | 0.065 | 0.35 | 0.001 | 0 |
| mem_ctrl_alu2 | 0.029 | 0.031 | 0.051 | 0.072 | 0 | 0.233 | 0.498 | 0 | 0 |
| priority_alu2 | 0.008 | 0.018 | 0.051 | 0.001 | 0.062 | 0.062 | 0.35 | 0.001 | 0 |
| router_alu2 | 0.195 | 0.187 | 0.203 | 0.158 | 0.266 | 0.161 | 0.049 | 0.049 | 0 |
| | | | | | | | | | |
| adder | 0.124 | 0.12 | 0.156 | 0.079 | 0.255 | 0.014 | 0.25 | 0.014 | 1 |
| bar | 0.03 | 0.031 | 0.05 | 0.075 | 0.001 | 0.236 | 0.508 | 0.001 | 0 |
| square | 0.027 | 0.047 | 0.094 | 0.016 | 0.068 | 0.108 | 0.385 | 0.016 | 1 |
| sqrt | 0.009 | 0.009 | 0.031 | 0.041 | 0.012 | 0.157 | 0.448 | 0.009 | 1 |

Table 12: Δ_{\cosine} on validation data (EPFL random control agent II). δ_{th} computed from AUROC curve: 0.005

| Validation benchmarks | $\Delta_{\cos}(h_{valid}, h_{train})$ | | | | | | | δ_{min} | Winner (0-MCTS+RL /1- MCTS) |
|-----------------------|---------------------------------------|-------|-------|-----------|----------|----------|-------|----------------|-----------------------------------|
| | arbiter | ctrl | i2c | int2float | mem_ctrl | priority | voter | | |
| arbiter_apex7 | 0 | 0.029 | 0.064 | 0.007 | 0.053 | 0.092 | 0.111 | 0 | 0 |
| ctrl_apex7 | 0.029 | 0.001 | 0.02 | 0.027 | 0.025 | 0.123 | 0.142 | 0.001 | 0 |
| i2c_apex7 | 0.069 | 0.023 | 0 | 0.062 | 0.051 | 0.153 | 0.176 | 0 | 0 |
| int2float_apex7 | 0.006 | 0.017 | 0.049 | 0.002 | 0.057 | 0.073 | 0.091 | 0.002 | 0 |
| mem_ctrl_apex7 | 0.053 | 0.031 | 0.051 | 0.072 | 0 | 0.233 | 0.259 | 0 | 0 |
| priority_apex7 | 0.015 | 0.047 | 0.088 | 0.005 | 0.108 | 0.042 | 0.055 | 0.005 | 0 |
| voter_apex7 | 0.02 | 0.055 | 0.097 | 0.004 | 0.121 | 0.034 | 0.047 | 0.004 | 0 |
| | | | | | | | | | |
| arbiter_alu2 | 0.001 | 0.022 | 0.054 | 0.006 | 0.047 | 0.09 | 0.11 | 0.001 | 1 |
| ctrl_alu2 | 0.024 | 0.002 | 0.024 | 0.018 | 0.037 | 0.096 | 0.113 | 0.002 | 0 |
| i2c_alu2 | 0.067 | 0.022 | 0 | 0.059 | 0.052 | 0.146 | 0.169 | 0 | 0 |
| int2float_alu2 | 0.006 | 0.017 | 0.049 | 0.001 | 0.059 | 0.065 | 0.082 | 0.001 | 0 |
| mem_ctrl_alu2 | 0.053 | 0.031 | 0.051 | 0.072 | 0 | 0.233 | 0.259 | 0 | 0 |
| priority_alu2 | 0.007 | 0.018 | 0.051 | 0.001 | 0.062 | 0.062 | 0.078 | 0.001 | 0 |
| voter_alu2 | 0.008 | 0.019 | 0.053 | 0.001 | 0.065 | 0.059 | 0.075 | 0.001 | 1 |
| | | | | | | | | | |
| adder | 0.123 | 0.12 | 0.156 | 0.079 | 0.255 | 0.014 | 0.012 | 0.012 | 1 |
| bar | 0.055 | 0.031 | 0.05 | 0.075 | 0.001 | 0.236 | 0.261 | 0.001 | 0 |
| square | 0.008 | 0.047 | 0.094 | 0.016 | 0.068 | 0.108 | 0.127 | 0.008 | 1 |
| sqrt | 0.037 | 0.009 | 0.031 | 0.041 | 0.012 | 0.157 | 0.177 | 0.009 | 1 |

Table 13: Δ_{cosine} on validation data (EPFL random control agent III). δ_{th} computed from AUROC curve: 0.007

| Validation benchmarks | $\Delta_{cos}(h_{valid}, h_{train})$ | | | | | | | δ_{min} | Winner (0-MCTS+RL /1- MCTS) |
|-----------------------|--------------------------------------|-------|-------|-----------|----------|--------|-------|----------------|-----------------------------|
| | arbiter | cavlc | i2c | int2float | mem_ctrl | router | voter | | |
| arbiter_apex7 | 0 | 0.013 | 0.064 | 0.007 | 0.053 | 0.359 | 0.111 | 0 | 0 |
| cavlc_apex7 | 0.014 | 0.001 | 0.032 | 0.016 | 0.022 | 0.402 | 0.136 | 0.001 | 0 |
| i2c_apex7 | 0.069 | 0.037 | 0 | 0.062 | 0.051 | 0.393 | 0.176 | 0 | 0 |
| int2float_apex7 | 0.006 | 0.008 | 0.049 | 0.002 | 0.057 | 0.339 | 0.091 | 0.002 | 1 |
| mem_ctrl_apex7 | 0.053 | 0.029 | 0.051 | 0.072 | 0 | 0.498 | 0.259 | 0 | 0 |
| router_apex7 | 0.249 | 0.286 | 0.292 | 0.236 | 0.366 | 0.022 | 0.229 | 0.022 | 0 |
| voter_apex7 | 0.02 | 0.037 | 0.097 | 0.007 | 0.121 | 0.317 | 0.047 | 0.007 | 0 |
| arbiter_alu2 | 0.001 | 0.008 | 0.054 | 0.006 | 0.047 | 0.361 | 0.11 | 0.001 | 0 |
| cavlc_alu2 | 0.012 | 0 | 0.034 | 0.013 | 0.027 | 0.398 | 0.125 | 0 | 0 |
| i2c_alu2 | 0.067 | 0.035 | 0 | 0.059 | 0.052 | 0.391 | 0.169 | 0 | 0 |
| int2float_alu2 | 0.006 | 0.007 | 0.049 | 0.001 | 0.059 | 0.35 | 0.082 | 0.001 | 0 |
| mem_ctrl_alu2 | 0.053 | 0.029 | 0.051 | 0.072 | 0 | 0.498 | 0.259 | 0 | 0 |
| router_alu2 | 0.171 | 0.195 | 0.203 | 0.158 | 0.266 | 0.049 | 0.173 | 0.049 | 0 |
| voter_alu2 | 0.008 | 0.008 | 0.053 | 0.001 | 0.065 | 0.351 | 0.075 | 0.001 | 1 |
| adder | 0.123 | 0.124 | 0.156 | 0.079 | 0.255 | 0.25 | 0.012 | 0.012 | 1 |
| bar | 0.055 | 0.03 | 0.05 | 0.075 | 0.001 | 0.508 | 0.261 | 0.001 | 0 |
| square | 0.008 | 0.027 | 0.094 | 0.016 | 0.068 | 0.385 | 0.127 | 0.008 | 1 |
| sqrt | 0.037 | 0.009 | 0.031 | 0.041 | 0.012 | 0.448 | 0.177 | 0.009 | 0 |

Table 14: Δ_{cosine} on validation data (EPFL random control agent IV). δ_{th} computed from AUROC curve: 0.015

| Validation benchmarks | $\Delta_{cos}(h_{valid}, h_{train})$ | | | | | | | | δ_{min} | Winner (0-MCTS+RL /1- MCTS) |
|-----------------------|--------------------------------------|-------|-------|-------|-----------|----------|--------|-------|----------------|-----------------------------|
| | arbiter | cavlc | ctrl | i2c | int2float | priority | router | voter | | |
| arbiter_apex7 | 0 | 0.013 | 0.029 | 0.064 | 0.3231 | 0.092 | 0.359 | 0.111 | 0 | 0 |
| cavlc_apex7 | 0.014 | 0.001 | 0.005 | 0.032 | 0.3618 | 0.117 | 0.402 | 0.136 | 0.001 | 1 |
| ctrl_apex7 | 0.029 | 0.006 | 0.001 | 0.02 | 0.3474 | 0.123 | 0.386 | 0.142 | 0.001 | 0 |
| i2c_apex7 | 0.069 | 0.037 | 0.023 | 0 | 0.3537 | 0.153 | 0.393 | 0.176 | 0 | 0 |
| int2float_apex7 | 0.016 | 0.018 | 0.017 | 0.049 | 0.3051 | 0.073 | 0.339 | 0.091 | 0.016 | 1 |
| priority_apex7 | 0.015 | 0.031 | 0.047 | 0.088 | 0.2826 | 0.042 | 0.314 | 0.055 | 0.015 | 0 |
| router_apex7 | 0.249 | 0.286 | 0.278 | 0.292 | 0.0108 | 0.218 | 0.012 | 0.229 | 0.011 | 0 |
| voter_apex7 | 0.012 | 0.037 | 0.055 | 0.097 | 0.2853 | 0.034 | 0.317 | 0.047 | 0.012 | 0 |
| arbiter_alu2 | 0.001 | 0.008 | 0.022 | 0.054 | 0.3249 | 0.09 | 0.361 | 0.11 | 0.001 | 0 |
| cavlc_alu2 | 0.012 | 0 | 0.006 | 0.034 | 0.3582 | 0.106 | 0.398 | 0.125 | 0 | 0 |
| ctrl_alu2 | 0.024 | 0.004 | 0.002 | 0.024 | 0.3393 | 0.096 | 0.377 | 0.113 | 0.002 | 0 |
| i2c_alu2 | 0.067 | 0.035 | 0.022 | 0 | 0.3519 | 0.146 | 0.391 | 0.169 | 0 | 0 |
| int2float_alu2 | 0.006 | 0.007 | 0.017 | 0.049 | 0.315 | 0.065 | 0.35 | 0.082 | 0.006 | 0 |
| priority_alu2 | 0.007 | 0.008 | 0.018 | 0.051 | 0.315 | 0.062 | 0.35 | 0.078 | 0.007 | 0 |
| router_alu2 | 0.171 | 0.195 | 0.187 | 0.203 | 0.0441 | 0.161 | 0.049 | 0.173 | 0.0441 | 0 |
| voter_alu2 | 0.008 | 0.008 | 0.019 | 0.053 | 0.3159 | 0.059 | 0.351 | 0.075 | 0.008 | 1 |
| adder | 0.123 | 0.124 | 0.12 | 0.156 | 0.225 | 0.019 | 0.25 | 0.016 | 0.019 | 1 |
| bar | 0.055 | 0.03 | 0.031 | 0.05 | 0.4572 | 0.236 | 0.508 | 0.261 | 0.03 | 1 |
| square | 0.008 | 0.027 | 0.047 | 0.094 | 0.3474 | 0.108 | 0.386 | 0.127 | 0.008 | 0 |
| sqrt | 0.037 | 0.009 | 0.009 | 0.031 | 0.4032 | 0.157 | 0.448 | 0.177 | 0.009 | 0 |

Table 15: Δ_{cosine} on validation data (EPFL random control agent V). δ_{th} computed from AUROC curve: 0.005

| Validation benchmarks | $\Delta_{cos}(h_{valid}, h_{train})$ | | | | | | | δ_{min} | Winner (0-MCTS+RL /1- MCTS) |
|--------------------------|--------------------------------------|-------|-------|----------|----------|--------|-------|----------------|-----------------------------------|
| | arbiter | cavlc | ctrl | mem_ctrl | priority | router | voter | | |
| arbiter_apex7 | 0.011 | 0.013 | 0.029 | 0.053 | 0.092 | 0.359 | 0.111 | 0.011 | 1 |
| cavlc_apex7 | 0.014 | 0.001 | 0.005 | 0.022 | 0.117 | 0.402 | 0.136 | 0.001 | 0 |
| ctrl_apex7 | 0.029 | 0.006 | 0.01 | 0.025 | 0.123 | 0.386 | 0.142 | 0.006 | 1 |
| mem_ctrl_apex7 | 0.053 | 0.029 | 0.031 | 0 | 0.233 | 0.498 | 0.259 | 0 | 0 |
| priority_apex7 | 0.015 | 0.031 | 0.047 | 0.108 | 0.005 | 0.314 | 0.055 | 0.005 | 0 |
| router_apex7 | 0.249 | 0.286 | 0.278 | 0.366 | 0.218 | 0.01 | 0.229 | 0.01 | 0 |
| voter_apex7 | 0.02 | 0.037 | 0.055 | 0.121 | 0.034 | 0.317 | 0.004 | 0.004 | 0 |
| arbiter_alu2 | 0.001 | 0.008 | 0.022 | 0.047 | 0.09 | 0.361 | 0.11 | 0.001 | 0 |
| cavlc_alu2 | 0.012 | 0 | 0.006 | 0.027 | 0.106 | 0.398 | 0.125 | 0 | 0 |
| ctrl_alu2 | 0.024 | 0.014 | 0.006 | 0.037 | 0.096 | 0.377 | 0.113 | 0.006 | 1 |
| mem_ctrl_alu2 | 0.053 | 0.029 | 0.031 | 0 | 0.233 | 0.498 | 0.259 | 0 | 0 |
| priority_alu2 | 0.007 | 0.008 | 0.018 | 0.062 | 0.062 | 0.35 | 0.078 | 0.007 | 1 |
| router_alu2 | 0.171 | 0.195 | 0.187 | 0.266 | 0.161 | 0.049 | 0.173 | 0.049 | 0 |
| voter_alu2 | 0.008 | 0.008 | 0.019 | 0.065 | 0.059 | 0.351 | 0.075 | 0.008 | 1 |
| adder | 0.123 | 0.124 | 0.12 | 0.255 | 0.014 | 0.25 | 0.012 | 0.012 | 1 |
| bar | 0.055 | 0.03 | 0.031 | 0.001 | 0.236 | 0.508 | 0.261 | 0.001 | 0 |
| square | 0.008 | 0.027 | 0.047 | 0.068 | 0.108 | 0.385 | 0.127 | 0.008 | 1 |
| sqrt | 0.037 | 0.009 | 0.004 | 0.012 | 0.157 | 0.448 | 0.177 | 0.004 | 0 |